

Common environmental stress responses in a model marine diatom

Zhengke Li^{1,2} , Yong Zhang^{2,3} , Wei Li⁴ , Andrew J. Irwin⁵  and Zoe V. Finkel² 

¹School of Biological and Pharmaceutical Sciences, Shannxi University of Science and Technology, Xi'an, Shannxi, 710021, China; ²Department of Oceanography, Dalhousie University, 1355 Oxford Street, Halifax, NS, B3H 4R2, Canada; ³College of Environmental Science and Engineering, Fujian Normal University, Fuzhou, Fujian, 350007, China; ⁴College of Life and Environmental Sciences, Huangshan University, Huangshan, Anhui, 245041, China; ⁵Department of Mathematics & Statistics, Dalhousie University, 1355 Oxford Street, Halifax, NS, B3H 4R2, Canada

Author for correspondence:

Zhengke Li

Email: zkli@dal.ca

Received: 22 December 2022

Accepted: 30 June 2023

New Phytologist (2023)

doi: 10.1111/nph.19147

Key words: diatom, environmental stress responses, photosynthesis, *Thalassiosira pseudonana*, transcriptomics.

Summary

- Marine planktonic diatoms are among the most important contributors to phytoplankton blooms and marine net primary production. Their ecological success has been attributed to their ability to rapidly respond to changing environmental conditions.
- Here, we report common molecular mechanisms used by the model marine diatom *Thalassiosira pseudonana* to respond to 10 diverse environmental stressors using RNA-Seq analysis.
- We identify a specific subset of 1076 genes that are differentially expressed in response to stressors that induce an imbalance between energy or resource supply and metabolic capacity, which we termed the diatom environmental stress response (d-ESR). The d-ESR is primarily composed of genes that maintain proteome homeostasis and primary metabolism. Photosynthesis is strongly regulated in response to environmental stressors but chloroplast-encoded genes were predominantly upregulated while the nuclear-encoded genes were mostly downregulated in response to low light and high temperature.
- In aggregate, these results provide insight into the molecular mechanisms used by diatoms to respond to a range of environmental perturbations and the unique role of the chloroplast in managing environmental stress in diatoms. This study facilitates our understanding of the molecular mechanisms underpinning the ecological success of diatoms in the ocean.

Introduction

Marine diatoms contribute *c.* 40% of marine primary production and particulate carbon export (Falkowski *et al.*, 1998; Field *et al.*, 1998; Tréguer *et al.*, 2018) and are among the most ecologically successful phytoplankton in the ocean (De La Rocha & Passow, 2004). Planktonic diatoms drift with the ocean currents and therefore are subject to rapid environmental variation, including changes in irradiance, temperature, pH, nutrient availability, and reactive oxygen stress (ROS; Boyd *et al.*, 2019). Diatom blooms are often associated with large changes in pH, light, and nutrient availability. Among phytoplankton, diatoms appear to be especially well adapted to variable conditions and it is hypothesized that their stress response mechanisms may contribute to their ecological success. While transcriptomic studies have been successfully used to identify molecular mechanisms used by diatoms to respond to specific, individual stressors such as nitrogen (Mock *et al.*, 2008; Hockin *et al.*, 2012; Abida *et al.*, 2015; Alexander *et al.*, 2015; Alipanah *et al.*, 2015; Levitan *et al.*, 2015; Remmers *et al.*, 2018), phosphorous (Dyhrman *et al.*, 2012; Alexander *et al.*, 2015; Cruz de Carvalho *et al.*, 2016; Zhang *et al.*, 2016), silicon (Mock *et al.*, 2008; Sapriel *et al.*, 2009;

Shrestha *et al.*, 2012; Smith *et al.*, 2016), iron (Allen *et al.*, 2008; Mock *et al.*, 2008), high light (Nymark *et al.*, 2009; Park *et al.*, 2010), temperature (Mock *et al.*, 2008; Liang *et al.*, 2019), pH, and CO₂ (Mock *et al.*, 2008; Hennon *et al.*, 2015; Li *et al.*, 2015) change, here we identify the common molecular responses used by a model diatom to respond to many environmental stressors.

Transcriptomic investigations of model organisms such as yeast indicate that eukaryotes may have a common set of genes that are expressed in response to diverse environmental stressors (the common environmental stress response, CESR; Gasch *et al.*, 2000; Causton *et al.*, 2001; Chen *et al.*, 2003). Genes and their promoters that respond to only one or a few specific stressors are not included in the CESR, but instead can be used as markers of distinctive stress responses. In yeast, approximately one-third of the genes in the CESR are induced while two-thirds are repressed. Induced genes are involved in pathways associated with protein folding and degradation, DNA damage repair, ROS detoxification, and autophagy, while many repressed genes are associated with ribosomes and RNA metabolism. The regulatory controls of the CESR in yeast have not been fully elucidated but Msn2/Msn4, or Sty1p and Atf1p have been implicated (Causton

et al., 2001; Chen *et al.*, 2003). Neither the common stress response nor their regulatory controls have been identified in diatoms.

Physiological, proteomic, and transcriptomic studies on eukaryotic phytoplankton indicate they might have a common molecular response to multiple environmental stressors. For example, Si and Fe limitation induced 84 common genes in the diatom *Thalassiosira pseudonana* (Mock *et al.*, 2008). On the contrary, contrasting physiological responses have been reported for high-light or low-temperature conditions compared with low-light or high-temperature conditions, such as Chl *a* content, PSII excitation pressure, and the functional absorption cross-section of PSII (Huner *et al.*, 1998; Li *et al.*, 2020). Light absorption, excitation energy transfer, and primary photochemistry in photosynthesis are temperature-independent (Raven & Geider, 1988), but biochemical reactions and therefore cell metabolism are temperature-dependent (Gillooly *et al.*, 2001). Consequently, low-temperature and high-light conditions can cause an oversupply of energy from light absorption relative to metabolic capacity in photosynthetic organisms, facilitating superoxide anion radical (O_2^-) or singlet oxygen (1O_2) formation and oxidative damage (Maxwell *et al.*, 1994; Huner *et al.*, 1998). By contrast, high-temperature, low-light, and nutrient-starvation conditions can reduce resource and energy supply relative to metabolic requirements, resulting in a cellular energy deficit (Huner *et al.*, 1998). We hypothesize that stressors that stimulate an excess of energy relative to metabolic capacity should induce contrasting transcriptomic responses compared with stressors that limit metabolic capacity by reduced resource supply. While the fundamental pathways induced by stress may be common across eukaryotes, we anticipate additional complexity in the stress response of photosynthetic organisms and perhaps differences across eukaryotes with chloroplasts with different evolutionary origins.

Chloroplasts are semi-autonomous organelles with a small number of protein-coding genes (Timmis *et al.*, 2004; Oudot-Le Secq *et al.*, 2007). Chloroplasts are a source of ROS, especially when light absorption exceeds metabolic capacity and the chloroplast is damaged due to resource limitation, high light, or temperature conditions (Takahashi & Murata, 2008; Gill & Tuteja, 2010; Sharma *et al.*, 2012; Järvi *et al.*, 2015). Since they are central to diatom metabolism, chloroplasts must be tightly controlled and quickly repaired and can be expected to feature prominently in response to environmental stressors. Diatoms arose from a secondary endosymbiotic event and have a highly reduced plastid genome and distinctive evolutionary history compared with green algae and higher plants (Prihoda *et al.*, 2012). Genes may have been retained in the plastid because of their importance in maintaining redox balance, their high turnover rates, and consequent need for tight regulation relative to the redox state of the plastid (Nisbet *et al.*, 2004). Another distinctive feature of diatoms is their obligate requirement for Si and the cell-cycle checkpoint that arrests cell division in the absence of Si, which can be expected to lead to a unique stress response (Martin-Jézéquel *et al.*, 2000; Mock *et al.*, 2008; Smith *et al.*, 2016).

To study the environmental stress response in diatoms and test these hypotheses, we cultured the model marine diatom *T. pseudonana* CCMP1335 (Armbrust *et al.*, 2004) under many stress conditions that diatoms experience *in situ*, including different types of nutrient starvation (N, P, Fe, and Si), increases and decreases in light and temperature, and pH changes likely to be associated with ocean acidification (7.8 vs 8.1) and analyzed changes in the transcriptome relative to control treatments (optimal, exponential growth conditions) over 0–72 h. We included an exogenous ROS treatment created by the addition of H_2O_2 as a positive control to quantify the impact of ROS independent of another stressor. We clustered genes and pathways based on patterns of differential expression across these stressors to identify stress responses common across all, or subsets of different types of stress conditions, and highlight especially enriched Kyoto Encyclopedia of Genes and Genomes (KEGG) pathways. A systematic analysis reveals a complexity in the stress response in diatoms not observed in yeast, which we attribute to their distinctive evolutionary history and the complexity of energy, redox state, and organelle management.

Materials and Methods

Strain and culture conditions

The coastal diatom *T. pseudonana* (Hustedt) Hasle et Heimdal (CCMP 1335) was obtained from the Bigelow National Center for Marine Algae and Microbiota. Cultures were maintained in 250 ml polycarbonate bottles with 250 ml modified ESAW medium (Berges *et al.*, 2001) at pH 8.1 and 20°C with a continuous illumination of 100 $\mu\text{mol photons m}^{-2} \text{s}^{-1}$ for over 20 generations in the mid-exponential growth phase. We used continuous light to simplify the experimental design and to minimize the impact of diurnal forcings imposed by a photoperiod on the transcriptome (Becker *et al.*, 2021; Muratore *et al.*, 2022). Note the continuous light treatment used here lacks both short-term light fluctuations and a light–dark cycle. Acclimated cultures were then exposed to 10 experimental stress treatments: four types of nutrient-starvation, N-, P-, Si-, and Fe-free media, a high (26°C, referred to as HT) and low-temperature (14°C, LT) treatment, a low-light (LL) and a high-light treatment (HL; 10 and 800 $\mu\text{mol photons m}^{-2} \text{s}^{-1}$), a low-pH treatment (pH 7.8, LpH; all other treatments were maintained at pH 8.2) set by using 16 mM N-(2-hydroxyethyl)-piperazine-N9-2-propanesulfonic acid (EPPS; Sigma-Aldrich) adjusted with ultra-pure HCl/NaOH, and a reactive oxygen species (ROS) treatment created by an initial exogenous addition of H_2O_2 (Sigma) at a final concentration of 0.165 mM achieved in the acclimated ESAW media before the cells were transferred from the stock culture (Supporting Information Table S1). Before the experiment, extensive preliminary experiments were conducted to identify our temperature, light, and H_2O_2 treatments, the ideal initial cell density for sampling, and EPPS concentration to maintain a stable pH across all treatments for the duration of the full experiment. Control bottles were sampled at the same time points (0, 2, 6, 24, and 72 h) with treatments to allow us to account for the impact of sample handling. Cell concentrations were monitored

using a Z2 Coulter Counter (Beckman Coulter, Fullerton, CA, USA) with Coulter Z2 ACCUCOMP software. Each control and experimental treatment was started with a different cell density, chosen based on pre-experimental work, to achieve a final cell density of $c. 5 \times 10^5$ cells ml^{-1} at all the sampling times (0, 2, 6, 24, and 72 h). All experiments were run with four independent biological replicate bottles. Additional experimental detail is provided in Table S1 and previous publications that document housekeeping genes and photophysiological responses from this experiment (Li *et al.*, 2020, 2022).

Sampling, RNA extraction, and sequencing

Cells were collected by gentle filtration onto polycarbonate Millipore membrane filters (pore size: 0.8 μm , diameter: 25 mm), then frozen in liquid nitrogen, and stored at -80°C until further analysis. Total RNA was extracted using TRIzol reagent (Invitrogen) and RNeasy Plus Mini Kit (Qiagen) with a phenol-chloroform method (Lin *et al.*, 2012). A gDNA eliminator column (RNeasy Plus Mini Kit) and Qiagen's RNase-free DNase Set (an on-column treatment) were used to remove gDNA according to the manufacturer's instructions. All RNA samples passed the RNA integrity analysis conducted by Génome Québec Innovation Centre (Agilent 2100 Bioanalyzer; Agilent Technologies, Palo Alto, CA, USA), had concentrations of 100 $\text{ng } \mu\text{l}^{-1}$, and $\text{A260/A280} \geq 2.1$ and $\text{A260/A230} \geq 2.4$ (NanoDrop ND-1000 Spectrophotometer, Wilmington, DE, USA), and were sequenced by Illumina HiSeq 6000 at the Genome Quebec Innovation Centre with an Illumina TruSeq Stranded mRNA Library preparation method (paired-end 100 bp reads). All raw read files (detailed descriptions of these files are provided in Dataset S1) are available through NCBI SRA (BioProject: PRJNA734969).

Bioinformatic analyses

The quality and contamination of the raw reads were checked using FASTQC v.0.11.8 (Andrews, 2010) and FASTQ SCREEN v.0.13.0 (Wingett & Andrews, 2018) and inspected using MULTIQ (Ewels *et al.*, 2016). Quality trimming of the reads was performed with TRIMMOMATIC v.0.38 (Bolger *et al.*, 2014) with parameters set at ILLUMINACLIP:TruSeq3-PE.fa:2:30:10, LEADING:3, TRAILING:3, MINLEN:41, AVGQUAL:20, SLIDINGWINDOW:4:15, and HEADCROP:11 to remove low-quality bases and adapter sequences. Trimmed reads were mapped to the *T. pseudonana* CCMP 1335 transcript sequence data (NCBI, assembly ASM14940v2) using SALMON v.0.9.1 (Patro *et al.*, 2017) for the read count estimation. The mapping rates range between 95.6% and 97.8% for 22 selected samples (Fig. S1). To assess the differential expression, we compared expressions at $t = 2, 6, 24,$ and 72 h for each environmental treatment with the control at the same time. Normalized gene/KEGG Ortholog (KO) abundances, fold change values, and Benjamini–Hochberg adjusted P -value were calculated using DESEQ2 v.1.24.0 (Love *et al.*, 2014). Genes/KOs were identified as differentially expressed if they have a Benjamini–Hochberg adjusted P -value < 0.01 (Dataset S2, S3). Data analysis and

visualizations were made using R v.3.6.1 (R Development Core Team, 2013) and packages GGLOT2 v.3.2.0 (Wickham, 2016) and PHEATMAP v.1.0.12 (Kolde, 2012).

KEGG enrichment analysis and the hierarchical clustering of KEGG pathways

Four categories (i.e. metabolism, genetic information processing, environmental information processing, and cellular processes) of KEGG pathways and Brite hierarchies were selected for KEGG enrichment analyses. Pathways with more than six annotated KEGG Orthology identifiers (KO IDs) were selected for calculation. The P -value associated with the enrichment analysis was calculated by using a standard hypergeometric distribution test (Karp *et al.*, 2021); a pathway with an adjusted P -value ≤ 0.05 (Benjamini & Hochberg, 1995) was identified as a significantly enriched pathway (Dataset S4). Hierarchical clusters of enriched pathways were identified (1 for enriched up, -1 for enriched in downregulated genes, and 0 for nonenriched pathways) using R package GGLOT2 v.3.2.0 (Wickham, 2016) and PHEATMAP v.1.0.12 (Kolde, 2012).

Definition of d-ESR genes and d-ESR pathways

We identified a gene as part of the diatom environmental stress response (d-ESR) if it was upregulated at one or more time points in each of the N, P, Si, Fe, LL, and HT treatments and downregulated at one or more time points in both the HL and LT treatments, or the reverse (downregulated in N, P, Se, Fe, LL, and HT and upregulated in HL and LT). We refer to the subset of these genes that are upregulated in HL and LT as genes responsive to energy overload and the subset of these genes that are downregulated in HL and LT as genes responsive to metabolic-resource limitation (Dataset S2). Very few pathways are significantly enriched in upregulated genes at one or more time points in each of the N, P, Si, Fe, LL, and HT treatments and downregulated at one or more time points in both the HL and LT treatments, or the reverse (downregulated in N, P, Se, Fe, LL, and HT and upregulated in HL and LT). We therefore relaxed the criteria for d-ESR pathways. Pathways were identified as part of the d-ESR if they were enriched in upregulated genes at one or more time points under at least three of the N-, P-, Si-, Fe-starvation, low-light, and high-temperature treatments and enriched in downregulated genes at one or more time points under at least one of the high-light and low-temperature treatments, or the reverse (downregulated in N-, P-, Si-, Fe-starvation, low-light, and high-temperature treatments and upregulated in high-light and low-temperature treatments).

Genes linked to oxidative stress

Genes were identified as part of the ROS stress response if they were differentially expressed in each of the ROS, LL, LT, HL, and HT treatments at 2, 6, or 24 h, and each of N, P, Si, and Fe treatments at 24 or 72 h (Dataset S2). These time points were selected because cultures had largely recovered from the ROS

treatment at 72 h, there was a partial recovery in response to the light and temperature stressors at 72 h, and the full effects of nutrient starvation often took > 6 h to be expressed.

Supplemental methods and analyses

The supplement has methods for analyses of a mapping rate test of RNA-seq samples, the correlation between KEGG pathways, a comparison of the common set of genes induced by both Si starvation and Fe starvation reported in Mock *et al.* (2008) and this study, an analysis of the d-ESR genes with unknown function, gene co-expression module identification (WGCNA), *Cis*-regulatory element identification, TFs, and hub genes distribution analysis, a comparison of CESRs between diatoms and yeast, and a re-clustering of yeast data.

Results

Common patterns of differential gene expression across stress treatments in *T. pseudonana*

There was a complex pattern of differentially expressed genes (DEGs) in response to the environmental stressors (40 treatments, 10 stressors, and 4 time points). Of *T. pseudonana*'s 11 673 genes, 11 087 were differentially expressed in at least 4 of the 10 stressors (Datasets S2, S5).

The majority of the nutrient-starvation treatments (not including some of the early time points), plus the low-light and high-temperature treatments had a common response across many genes (cluster 1, Figs 1, S2). The ROS treatment (2–24 h), which we anticipated might be broadly similar to the stress response across all treatments, exhibited the largest number of DEGs with a pattern of up- and downregulation distinct from all other treatments (cluster 2, Fig. 1). A third pattern of differential expression was exhibited by the high-light and low-temperature treatments and treatments with relatively minor impacts on differential gene expression (Si-starvation at 2 h, P- and Fe-starvation at 2 and 6 h, and low-pH, cluster 3 in Fig. 1).

A subset of the DEGs were regulated in the opposing directions across clusters 1 and 3. We identified 1076 genes that were consistently up or consistently downregulated at one or more time points in each of the nutrient-starvation, low-light and high-temperature treatments and regulated in the opposite direction in both the high-light and low-temperature treatments (Fig. 1, see the [Materials and Methods](#) for details). We term the subset of these genes that are upregulated in both high-light and low-temperature conditions as the energy-overload response. By contrast, we refer to the subset of these genes that were upregulated in nutrient-stress, low-light, and high-temperature conditions as reflecting a metabolic-resource-limitation response. We refer to the combined set of these genes as the d-ESR (Table S2; Dataset S2). We identified 171 of 1071 d-ESR genes that had no GO, KEGG, and domain annotations (Fig. S3a). In a search for orthologs of the 171 genes among 26 species, we found many genes were more likely to be found to diatoms than more distantly related species (Fig. S3c).

The DEG response under the ROS treatments (2–24 h) had some similarities with both the energy overload and the metabolic-resource stress responses. For example, the aminoacyl-tRNA biosynthesis, ribosome, and amino acid biosynthesis-related pathways were enriched in downregulated genes in response to ROS, the nutrient-starvation, low-light and high-temperature treatments, but enriched in upregulated genes in response to most the low-temperature and high-light treatments (Figs 2, 3a, S4). By contrast, the proteasome pathway was enriched in upregulated genes in response to the ROS and low temperature and enriched in downregulated genes in response to most of the nutrient-starvation, low-light and high-temperature treatments (Fig. 3a).

We compared the common set of genes induced by both Si starvation and Fe starvation in Mock *et al.* (2008) with this study (Fig. S5). We observed a high degree of consistency of up-regulation, with a similar magnitude of differential expression, under Si- and Fe starvation between the studies, supporting the reliability of our dataset. Our data showed that other environmental stressors (P starvation, ROS, LL, HT, and even the last time point of LpH) also stimulated differential expression of many of these genes, indicating that these 'Si- and Fe starvation commonly induced genes' are not only common to Si- and Fe starvation but also to other stressors that Mock *et al.* (2008) did not assess.

Enriched pathways contributing to the d-ESR

There were six clusters of enriched KEGG pathways across the environmental stressors (Fig. S4). As with the gene expression, there was a common set of pathways that were enriched in response to the nutrient-starvation, low-light, and high-temperature treatments and enriched in the opposing direction (in up- vs downregulated genes) in response to the low-temperature and high-light treatments (predominately in clusters A with a few in clusters B and C; Figs 2, S4). Note that the d-ESR definition for pathways is relaxed relative to that for genes (see the [Materials and Methods](#)). Many of the enriched pathways in these clusters were associated with transcription and translation, transport and catabolism, folding sorting and degradation, and energy metabolism. Pathways associated with energy metabolism, such as photosynthesis and oxidative phosphorylation, are primarily in cluster B. The remaining three clusters of pathways (clusters D–F) have less pronounced patterns across the multiple stressors, but all pathways in cluster E are associated with cell growth and death or replication and repair and were predominately enriched under Fe-starvation and low-pH treatments (Fig. S4).

We identify 26 d-ESR-related pathways (Fig. 2). Many of the d-ESR metabolic-resource-limitation pathways were associated with autophagy and transport and catabolism and energy metabolism (Fig. 2, clusters C and B, respectively). The d-ESR energy-overload pathways were mainly associated with transcription and translation, amino acid metabolisms pathways in cluster A, and a few primary metabolism pathways in cluster B (Fig. 2; Table S2). Most of the d-ESR pathways and many of the enriched pathways in clusters A–C can be characterized as central

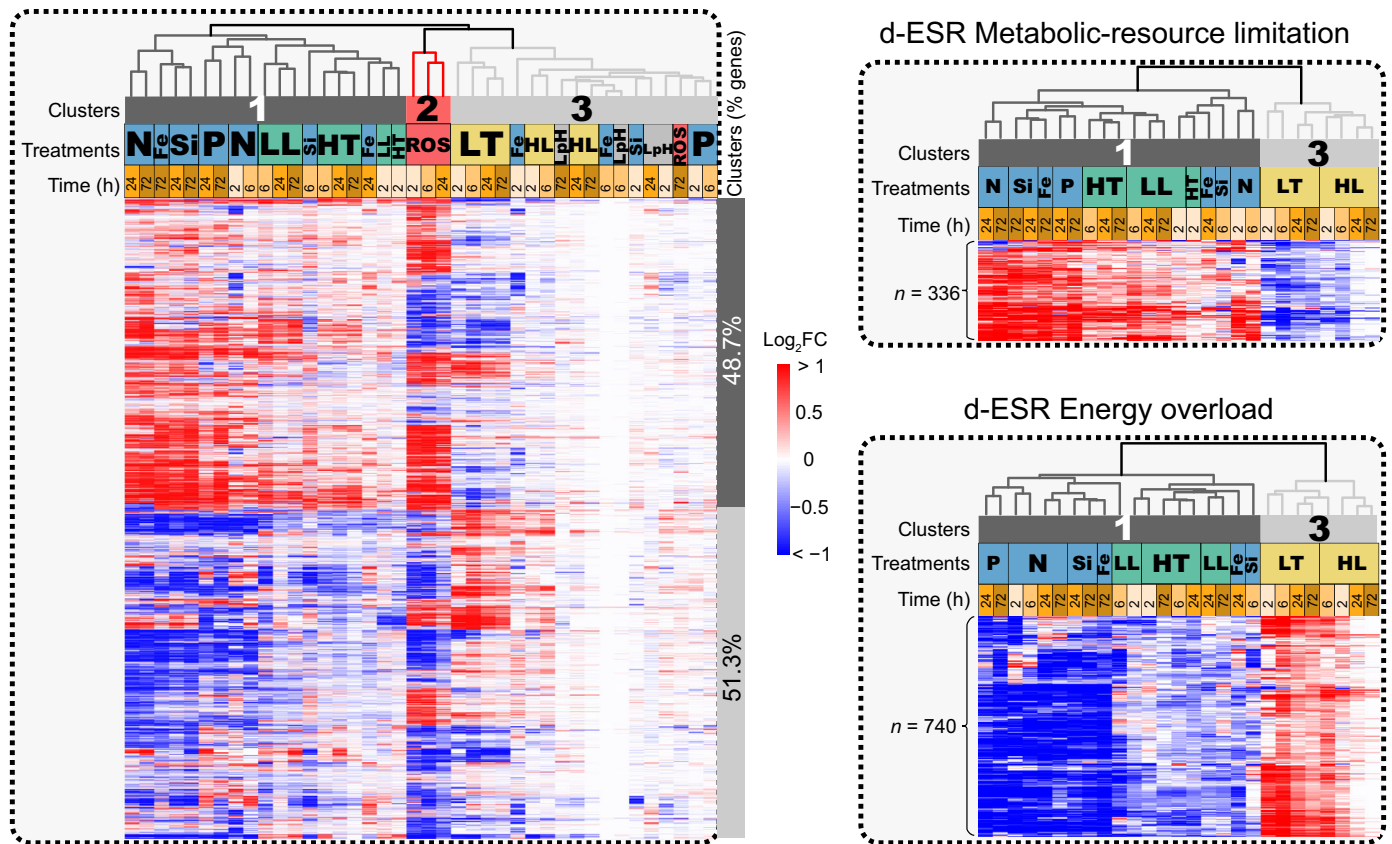


Fig. 1 Differential expression (\log_2FC) in *Thalassiosira pseudonana* (11 316 differentially expressed genes, left) and the diatom environmental stress response (d-ESR, right) in response to 10 environmental stressors. The environmental stressors form three main clusters (upper left dendrogram). Patterns of gene expression across treatments form two main clusters of 5511 genes (48.7%) and 5805 genes (51.3%). We define a d-ESR as the 336 genes that were upregulated in nutrient-stress, low-light, and high-temperature conditions (metabolic-resource limitation), and the 740 genes that were downregulated at one or more time points in each of the nutrient-starvation, low-light, and high-temperature treatments and regulated in the opposite direction in both the high-light and low-temperature treatments (energy overload). Treatments identified as nitrogen-starvation (N), phosphorus-starvation (P), silicon-starvation (Si), iron-starvation (Fe), low-light (LL), high-light (HL), low-temperature (LT), high-temperature (HT), low-pH (LpH), H_2O_2 (ROS) and the sampling time (2, 6, 24, and 72 h). ROS, reactive oxygen stress.

to maintaining energy-metabolic-protein homeostasis (Fig. 3a). Correlation of median expression across all 84 enriched pathways (not just the d-ESR related pathways) identified additional pathways that may participate in the d-ESR, such as the mTOR and AMPK signaling pathways, and confirmed that pathways associated with protein synthesis had a strongly correlated response across many of the environmental stressors and were negatively correlated with numerous pathways associated with catabolism (Fig. S6). Note that there are many genes that exhibit a d-ESR gene pattern of expression within pathways that do follow the d-ESR, examples associated with DNA replication, purine and pyrimidine metabolism, and carbon and lipid metabolism pathways are provided in Figs S7–S9.

Role of protein homeostasis in the d-ESR

Many of the differentially expressed genes and enriched pathways that contribute to the d-ESR are associated with protein homeostasis (Harper & Bennett, 2016; Figs 3, S10; Datasets S2, S6, S7). More specifically, amino acid biosynthesis, the ribosome, aminoacyl-tRNA biosynthesis, and many of the genes associated

with translation factors, amino acid-related enzymes, chaperones and folding catalysts, protein export, and some genes associated with protein processing in the ER were mostly downregulated in response to all the nutrient-starvation, low-light, and high-temperature treatments, but upregulated under the low-temperature and high-light treatments. By contrast, many of the genes associated with autophagy, including the lysosome (especially cathepsins; Datasets S2), and the ubiquitin-mediated proteolysis pathway were mostly upregulated in response to all the nutrient-starvation, low-light, and high-temperature treatments, but downregulated under low-temperature and high-light treatments (stresses that stimulate an energy surplus).

Within the protein homeostasis pathways, ribosome biogenesis is enriched and part of the d-ESR (Fig. 2); but not all the genes within the ribosome biogenesis pathway follow the d-ESR pattern (Figs 3b, S10). DEGs associated with ribosome assembly and maturation are mostly upregulated in response to the N-, Si-, Fe-starvation, low-light (24 h), ROS, low-temperature, and the high-light treatments (2–6 h) and downregulated in response to P-starvation, low-light (2–6 h), and high-temperature treatments. Genes involved in RNA modification (*NHP2*, *GARI*, *NOP10*,

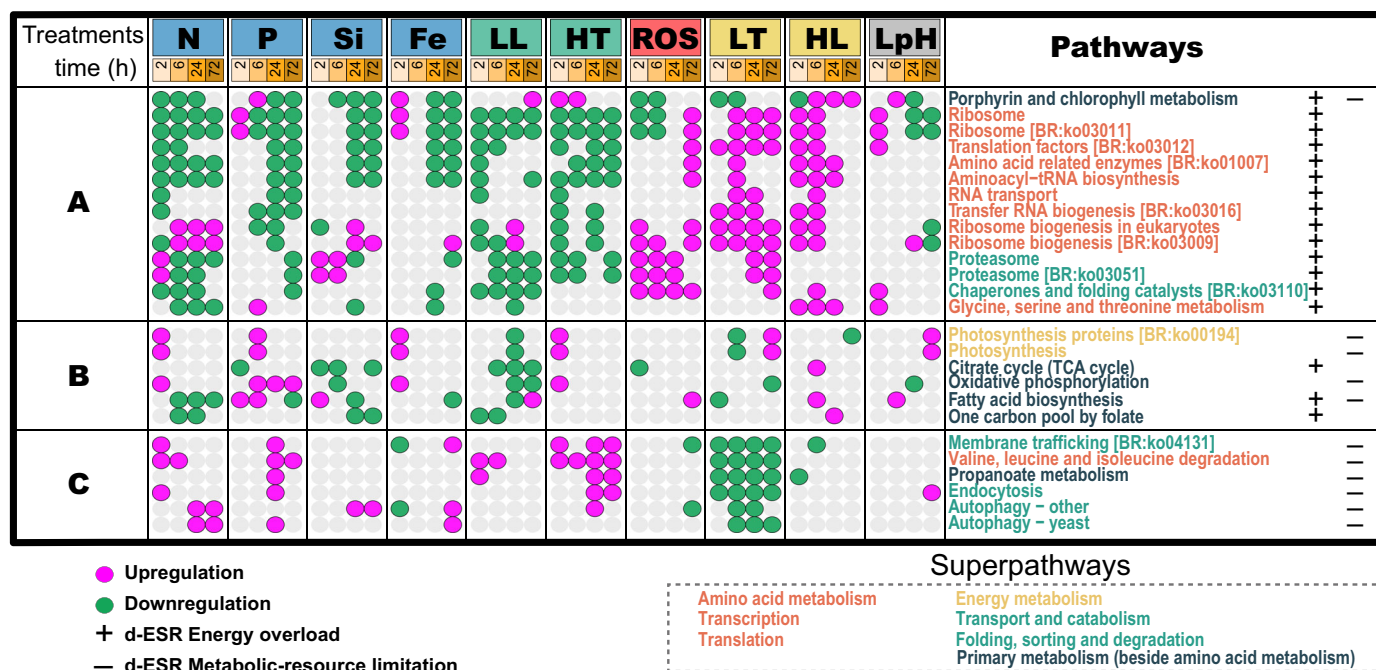


Fig. 2 Kyoto Encyclopedia of Genes and Genomes (KEGG) pathways in the diatom environmental stress response (d-ESR). Colored circles indicate a pathway that was enriched ($P < 0.05$) in up- (pink) or downregulated (green) genes at the corresponding treatment. d-ESR energy-overload pathways are labeled '+', and d-ESR metabolic-resource-limitation pathways are labeled '-'. Pathways are identified as part of super pathways with colored text according to the legend. Black bold capital letters on the left indicate clusters of enriched pathways. Treatments identified as nitrogen-starvation (N), phosphorus-starvation (P), silicon-starvation (Si), iron-starvation (Fe), low-light (LL), high-light (HL), low-temperature (LT), high-temperature (HT), low-pH (LpH), H_2O_2 (ROS), and the sampling time (2, 6, 24 and 72 h). The full set of 84 enriched pathways is in Supporting Information Fig. S4. ROS, reactive oxygen stress.

NOP56, *DKC1*, *NOP58*, *SNU13*, and *NOPI* are identified as part of/similar to the d-ESR (metabolic-resource limitation) and are predominately downregulated in response to the N-, Si-, Fe-starvation, and ROS as well as P-starvation, low-light, and the high-temperature treatments (Figs 3b, S10; Dataset S2). Almost all DEGs associated with the proteasome were upregulated under N- (2 h) and Si starvation (2–6 h), indicating they are not part of the d-ESR.

Impact of environmental stressors on DGE in photosynthesis

Photosynthesis is enriched in differentially expressed genes but is not part of the d-ESR, with genes similarly expressed under all nutrient-starvation treatments, ROS, LT, HL, and LpH with contrasting expression under LL and HT (Figs 2, 4, S11). Notably, genes have contrasting expression across the examined treatments between the nuclear- vs chloroplast-encoded genes in the photosynthesis pathway (Fig. 4a) and in all the photosynthesis-related pathways (Fig. 4b,c). The chloroplast-encoded genes, the PSI and PSII core, ATP synthase, *Cytb6f*, and *RBCL*, were mostly upregulated in response to all nutrient-starvation, ROS, low-pH, and low-temperature (24 h) treatments and downregulated under low-light (24–72 h) and low-temperature (6 h) treatments. An exception to this simple pattern is the nuclear-encoded gene *LHCb5* (Oudot-Le Secq *et al.*, 2007), which was upregulated under all stressors including low light. All 55 mapped chloroplast-encoded genes and genes in KEGG pathways associated with porphyrin and chlorophyll

metabolism and carbon fixation pathways generally adhere to a similar pattern (Fig. S11) with a few notable exceptions (Fig. S11; Dataset S2).

Potential regulators of the d-ESR

Several enriched global regulatory pathways, AMPK, TOR, the phosphatidylinositol signaling system, and acetyl-CoA pathways, exhibit expression patterns similar to the d-ESR with most of the observed deviations associated with the response to the light and temperature treatments for the AMPK complex (Fig. S12). In particular, there is a strong correlation between the d-ESR and the GATCR2 and TORC1 complex, RPS6 (phosphorylation target of TOR; Dobrenel *et al.*, 2016), branched-chain amino acid (BCAA) degradation (especially leucine), and some of the genes associated with fatty-acid degradation. Furthermore, the median expression of the BCAA degradation pathways is highly positively correlated with the median expression of DNA repair, proteolysis machinery associated with autophagy and the lysosome, amino acid and fatty-acid degradation, TOR, AMPK and the phosphatidylinositol signaling systems (Fig. S13). By contrast, pathways associated with amino acid, protein, and nucleic acid metabolism are negatively correlated with the BCAA degradation pathway (Fig. S13).

We found 26 putative transcription factors (TFs; De Geyter *et al.*, 2012) are associated with the d-ESR (Fig. S14; Dataset S2). The d-ESR metabolic-resource-limitation response is associated with TFs with 'cold-shock' DNA-binding domains. By contrast, the d-ESR energy-overload response is mainly characterized TFs

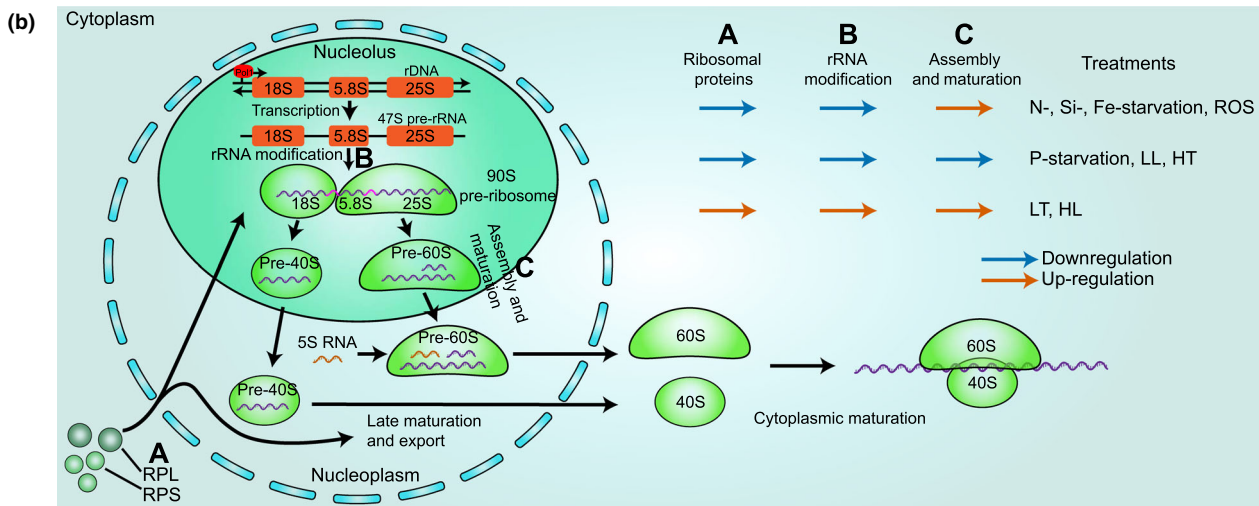
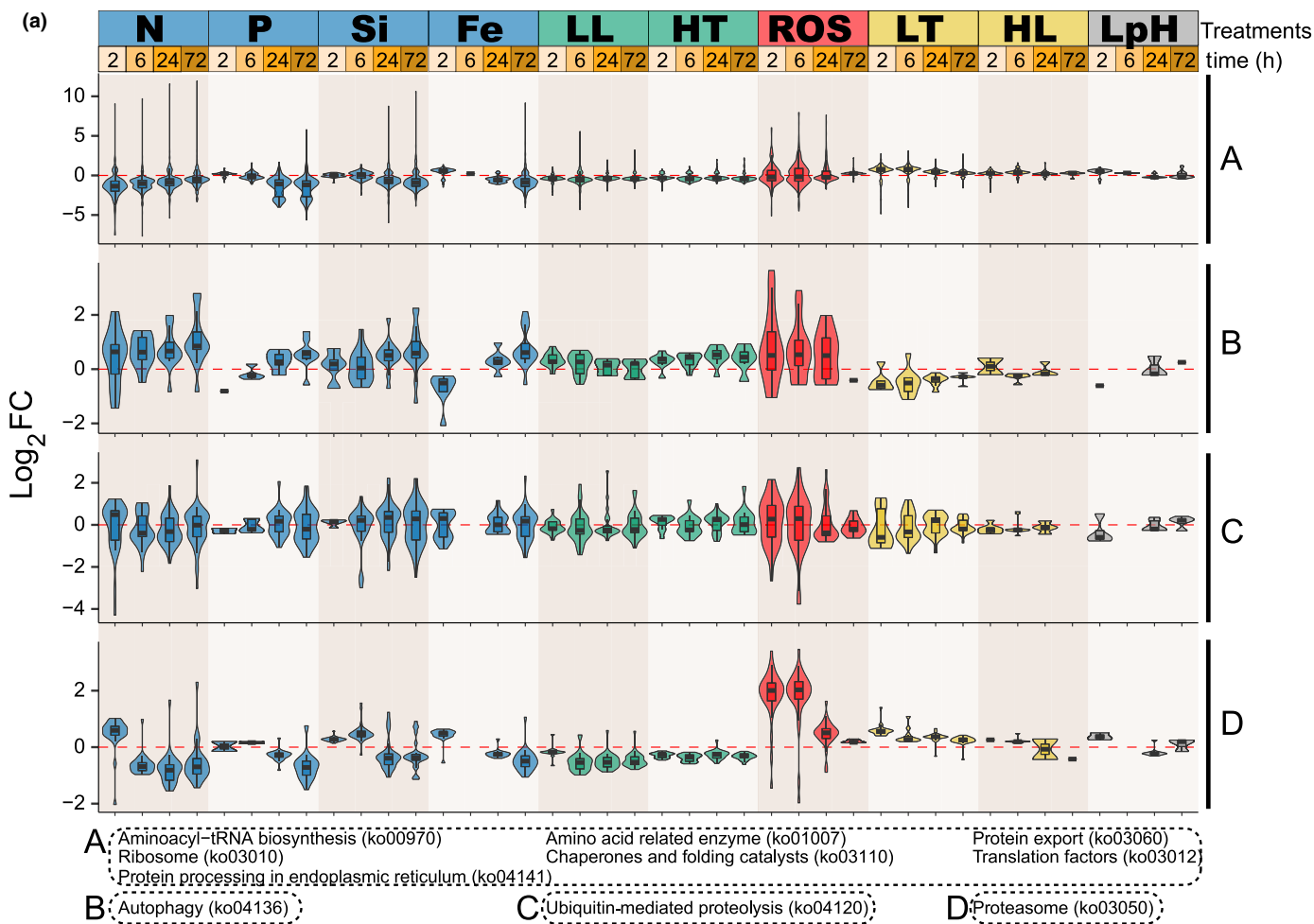


Fig. 3 Transcriptional response of proteome-balance-related pathways to 10 environmental stressors. (a) The differential expression of genes associated with proteome-balance-related pathways in response to 10 environmental stressors. Horizontal dotted lines are guides to aid comparison of the log₂FC across treatments. The violin plots show the full distribution of the data. Data points outside whiskers in boxplots are not shown for better visualization. Treatments identified as nitrogen-starvation (N), phosphorus-starvation (P), silicon-starvation (Si), iron-starvation (Fe), low-light (LL), high-light (HL), low-temperature (LT), high-temperature (HT), low-pH (LpH), H₂O₂ (ROS), and the sampling time (2, 6, 24 and 72 h). (b) Model of ribosome biosynthesis and/or repair under different stressors. Blue and vermilion arrows represent the downregulation and up-regulation of genes, respectively, in the processing of ribosome biosynthesis. Black arrows indicate either transport or processing steps. rDNA, ribosomal DNA; RPS, proteins of the small ribosomal subunit; RPL, proteins of the large ribosomal subunit; ROS, reactive oxygen stress.

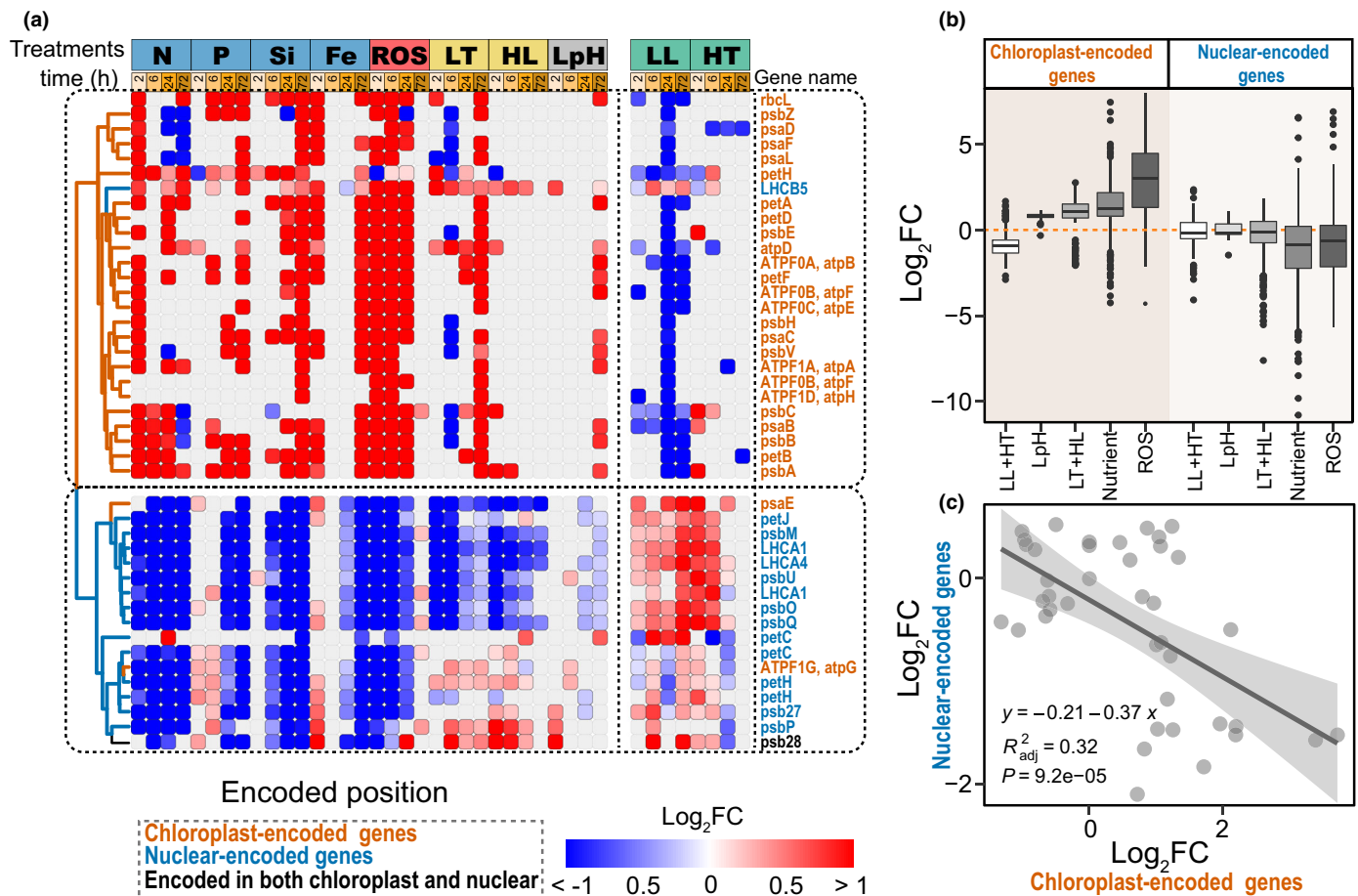


Fig. 4 Chloroplast-encoded genes and nuclear-encoded genes in photosynthesis exhibit distinct responses. (a) The differential expression (heatmap of log₂FC) of genes in the Kyoto Encyclopedia of Genes and Genomes (KEGG) photosynthesis pathway (ko00194) under 10 environmental stressors. Gene names are colored to indicate whether they are encoded in the nucleus (blue), chloroplast (vermillion), or both (black). Treatments identified as nitrogen-starvation (N), phosphorus-starvation (P), silicon-starvation (Si), iron-starvation (Fe), low-light (LL), high-light (HL), low-temperature (LT), high-temperature (HT), low-pH (LpH), H₂O₂ (ROS), and the sampling time (2, 6, 24, and 72 h). (b) A comparison of the differential expression of all selected photosynthesis-related genes between their encoded position under five groupings of the environmental treatments. Low-light and high-temperature (LL + HT), low-temperature and high-light (LT + HL), Nutrient (all four nutrient-starvation treatments), and ROS (H₂O₂). Horizontal dotted lines are guides to aid comparison of the log₂FC across treatments. Data are shown as boxplots with boxes showing the quartile values (25–75%) and the lines showing the medians. The whiskers extend to 1.5 times the interquartile range. Data beyond the whiskers represent outliers (black circles). (c) Linear correlation of the median differential expression between the chloroplast-encoded genes and the nuclear-encoded genes. The dark grey line is the regression line, the grey shading area is the 95% confident bands. Points represent 40 conditions (10 treatments × 4 time points). Genes used for analysis in (b) and (c) can be found in Supporting Information Fig. S11. ROS, reactive oxygen stress.

with HSF-type DNA-binding, zinc fingers, and Myb-like DNA-binding domains. Using a WGCNA co-expression analysis (method provided in the Supporting Information), we identified 24 TFs that may act as hub genes within modules of expression in response to environmental stressors (Fig. S15). Among them, two TFs, a zinc finger (*THAPSDRAFT_24580*) and a SNF (N-terminal domain; *THAPSDRAFT_2263240*), are also identified as d-ESR genes (Fig. S15). Putative TF-binding sites (TFBS) of WGCNA module genes were identified (Fig. S16).

Comparing the ESR of *T. pseudonana* to *S. cerevisiae*

We compared the gene and pathway enrichment patterns in *Saccharomyces cerevisiae* and *T. pseudonana* exposed to diverse stressors (Figs S17, S18). Note that *S. cerevisiae* was exposed to a different panel of stressors (Gasch *et al.*, 2000) than

T. pseudonana, although both include temperature and resource stressors. The stress response of both organisms includes an enrichment of the ribosome, ribosome biogenesis, RNA polymerase and transport, the peroxisome, and some metabolic pathways such as BCAA degradation and fatty-acid degradation (although the sign of enrichment often varies). Our re-clustering of the *S. cerevisiae* microarray data reveals that high-temperature induced a similar pattern of expression to N and amino acid starvation, which differed from the pattern induced by oxidative stressors (Fig. S18), consistent with the expression pattern in *T. pseudonana* in response to related stressors.

Discussion

Pioneering work on yeast identified a common set of genes expressed in response to a range of stressors termed the CESR

(Gasch *et al.*, 2000; Causton *et al.*, 2001; Chen *et al.*, 2003). Photosynthetic organisms have the additional burden of balancing energy harvested from light absorption relative to metabolic capacity in response to environmental perturbation (Huner *et al.*, 1998). Photophysiological responses indicate that stressors that cause an excess of energy or ROS relative to metabolic or quenching capacity might induce contrasting transcriptomic responses to stressors that limit metabolic capacity via reduced resource supply relative to metabolic capacity (Li *et al.*, 2020). Here, we show that the model marine diatom *T. pseudonana*, in contrast to yeast, has no single common set of genes that are similarly up or downregulated in response to diverse environmental stressors. High-light and low-temperature stressors induced a similar transcriptomic response that contrasted with the response to low light, high temperature, and nutrient starvation. We refer to this gene set with this contrasting expression pattern as the diatom common environmental stress response (d-ESR; Fig. 1). Many of the enriched pathways associated with the d-ESR are related to maintaining protein homeostasis in response to energetic, resource, or metabolic perturbations (Figs 2, 3). Photosynthesis is enriched in differentially expressed genes in response to the environmental stressors, but chloroplast-encoded genes are regulated in opposition to genes encoded in the nucleus (Fig. 4). Unexpectedly, the transcriptomic response to ROS was quite dissimilar to all the other environmental stressors examined (Fig. 1).

The d-ESR principally reflects protein reallocation in response to energetic–metabolic imbalances caused by the environmental stressors. Environmental stressors that restrict metabolic capacity (nutrient-starvation, low-light, and the high-temperature treatment which increased metabolic rate and resource demand) stimulate an up-regulation of genes and pathways associated with the breakdown of macromolecules (autophagy and the lysosome) and downregulation of protein production (translation and protein export-related processes) in *T. pseudonana* (Figs 1, 3). By contrast, these same genes and pathways are regulated in the opposing direction in response to the high-light and low-temperature treatments that stimulate an energy surplus relative to metabolic demand (Figs 1, 3). Several key energy-balancing genes and pathways are part of the d-ESR (or exhibit patterns of gene expression similar to the d-ESR), including acetyl-CoA (Pietrocola *et al.*, 2015; Shi & Tu, 2015; Fig. S12), branched-chain amino acid degradation (Figs 2, S12, S17), fatty-acid degradation (also upregulated in yeast; Figs S12, S17), *G6PD* (provides NADPH in PPP; Fig. S8), ketogenesis (that supply fuel and ATP; Puchalska & Crawford, 2017; Fig. S9), alcohol fermentation and lactate production (both supply ATP; Fig. S8), membrane proteins degradation through endocytosis and vacuoles/lysosome (Jones *et al.*, 2012; Lang *et al.*, 2014; Müller *et al.*, 2015; Figs 3, S4; Datasets S2), DNA and nucleic acid biosynthesis, and high energy-consuming pathways such as DNA replication, purine, and pyrimidine metabolism (Fig. S7). Several key genes (e.g. *PEPCK*, *MDH1*, *MDH2*, *PK*, and *PYC*) that participate in gluconeogenesis and pyruvate metabolism and the regeneration of carbohydrate from noncarbohydrate sources also contribute to the d-ESR (Fig. S8; Dataset S2). In aggregate, these results indicate that environmental stressors that stimulate an

imbalance in energetic/proteomic/metabolic state induce the d-ESR to restore the homeostasis through large-scale mobilization and reallocation of intracellular resources through protein homeostasis and primary metabolism.

Imbalances in energetic–metabolic state may act as a trigger for the d-ESR but how eukaryotes sense and use signals to regulate the CESR remains debated. There is some evidence that AMPK, a key regulator sensing cellular energy status, can act to restore energy balance by switching on alternative catabolic pathways that generate ATP while switching off anabolic pathways and other processes consuming ATP (Lin & Hardie, 2018). Our transcriptional analysis reveals that light and temperature perturbations lead to differential expression of AMPK genes, lipid and BCAA metabolism, and the glyoxylate cycle, consistent with their role in responding to and regulating energetic/metabolic state in *T. pseudonana*. TOR has been identified as a conserved central regulatory hub in eukaryotes for coordinating energy, stress, and nutrient signals for maintaining cellular homeostasis (Rexin *et al.*, 2015; Dobrenel *et al.*, 2016). TOR controls cell growth by promoting anabolic processes, including translation, ribosome biogenesis, and transcription, and by acting as an antagonist for catabolic processes such as autophagy and mRNA degradation, and acting upon primary metabolism including the TCA cycle, glycerolipid metabolism, and TAG accumulation, and endocytosis (Crespo & Hall, 2002; MacGurn *et al.*, 2011; Xiong & Sheen, 2015; González & Hall, 2017; Pérez-Pérez *et al.*, 2017). Our transcriptional analysis identified several genes involved in the TOR and AMPK signaling pathways contributing to the d-ESR, including RAPTOR (Fig. S12). Given the established crosstalk between AMPK and TOR (Dobrenel *et al.*, 2016), we hypothesize TOR may collect an energy signal from AMPK under changes in light and temperature and sense metabolic signals, either directly or indirectly, in response to nutrient starvation and other stressors, to regulate metabolic responses via phosphorylation of downstream TFs (Fig. S14). Contrasting with many of the protein translation-related pathways, the ribosome biosynthesis pathway was not part of the d-ESR although it responded to most of the stressors (Fig. 3). Ribosome biosynthesis is the pathway by which cells construct the ribosome and is very energetically expensive (Schleif, 1967; Warner, 1999). Under resource-restricted conditions, to save energy, *Escherichia coli* and mice will repair damaged ribosomes by replacing ribosomal proteins instead of replacing the whole ribosome (Pulk *et al.*, 2010; Mathis *et al.*, 2017). In *T. pseudonana*, most genes in ribosome biosynthesis are downregulated in response to the environmental treatments that stimulate the largest energy crisis: P starvation, low light (except 24 h), and high temperature. In contrast to many of the other translation-related pathways, including the ribosome pathway, a substantial proportion of the genes associated with ribosome assembly and maturation in ribosome biosynthesis were upregulated in the N- (6–72 h), Si- (24–72 h), Fe-starvation (72 h), and ROS (2–24 h) treatments, but some genes associated with rRNA modification were downregulated (Figs 3b, S10). In aggregate, these results reveal an energy-saving mechanism in *T. pseudonana* similar to, but not identical to, that observed in *Escherichia coli* and mice.

Reactive oxygen species and the induction of antioxidants are commonly considered a general response and indicator of stress (Borowitzka, 2018). In *T. pseudonana*, external application of hydrogen peroxide to stimulate ROS stimulated a distinct transcriptomic response: some pathways were enriched as in the high-light and low-temperature treatments, while other pathways were enriched as in the resource-limitation and high-temperature treatments. Genes in glutathione biosynthesis were predominately upregulated in response to the ROS, high-light, and low-temperature treatments, and were predominately downregulated in response to low-light, high-temperature, and the nutrient-starvation treatments (Fig. S19; Dataset S2), suggesting the induction of antioxidants is associated with the oxidative but not the resource-limitation stressors. The proteasome, but not autophagy, was enriched in upregulated genes for the first 24 h of the ROS treatment (Fig. 3), indicating that the proteasome is responsible for the selective degradation of oxidized proteins in diatoms, similar to mammals (Davies, 2001; Aiken *et al.*, 2011; Shang & Taylor, 2011). In response to most of the environmental stressors, autophagy appears to be the more dominant mechanism controlling proteolysis in diatoms (Fig. 3). Proteasome activity has high ATP demand (Kwon & Ciechanover, 2017; Bard *et al.*, 2018). The downregulation of genes in proteasome in the later stages of the nutrient-starvation treatments and under low light and high temperature may reflect an energy-saving strategy that was not feasible under the ROS treatment.

Photooxidative stress appears to be the dominant factor determining expression in the photosynthesis pathway in response to environmental stressors (Fig. 4). Like many photophysiological responses (Li *et al.*, 2020), gene expression within the photosynthesis pathway exhibit a similar response to nutrient-starvation, low-temperature, and high-light stress that contrasts in sign to the response to low-light and high-temperature stress (Fig. 4). Of note, the sign of differential gene expression across the stressors is strongly affected by whether the gene is encoded in the nucleus or chloroplast. Chloroplast-encoded photosynthesis genes (including the PSI and PSII core, ATP synthase) tend to be upregulated in response to all the nutrient-starvation, ROS, and low-temperature (at 72 h) treatments and downregulated under low-light, and not differentially regulated in response to high-temperature, while the nuclear-encoded photosynthesis genes are predominately differentially expressed in the opposing direction. The downregulation of electron carriers and light-harvesting genes under the nutrient-starvation, ROS, low-temperature, and high-light treatments likely reflects a strategy to decrease excitation pressure in the chloroplast. By contrast, the expressional pattern under low light and high temperature indicates a reverse regulation. The differential expression of the chloroplast- vs the nuclear-encoded genes may reflect differences in damage, signaling, and priority for repair. The chloroplast is a potential source of ROS (Pogson *et al.*, 2008) and self-regulation inherently involves shorter distances that may facilitate more rapid regulation of redox signals for repair processes (Pfannschmidt *et al.*, 1999). There are both plastid and nuclear copies of *PSB28*, which may reflect an ongoing plastid-to-nucleus transfer (Armbrust *et al.*, 2004; Oudot-Le Secq *et al.*, 2007). Several

photosynthesis genes (*PSB27*, *PETC*, *PETH*, *ATPG*, and especially *PSBP*) exhibit parallel expression patterns with *PSB28* perhaps indicating that these genes have been transferred, or are transitioning, to the nucleus.

Diatoms often dominate phytoplankton communities when environmental conditions are especially variable, blooming in the upper water column during periods of rapid change in nutrient and reactive oxygen concentrations, light, temperature, and pH. It has been hypothesized that diatoms may have unique molecular and physiological strategies to cope with environmental stressors. The model marine diatom *T. pseudonana* has a complex set of transcriptomic responses to environmental stress depending on whether the stressor generates an excess of energy relative to metabolic capacity, metabolic limitation due to resource scarcity, or oxidative stress. There is a set of genes and pathways that were differentially expressed in opposing directions in response to energy overload vs resource limitation that we term the d-ESR. The d-ESR is primarily associated with re-establishing balance between energy and resource inputs, and metabolic demand in response to environmental perturbations. We hypothesize the d-ESR may be triggered by imbalances in energetic/metabolic state and/or redox state and regulated by TOR and associated TFs. The d-ESR and photosynthesis potentially support diatoms to efficiently respond to environmental perturbations and thrive under variable conditions.

Acknowledgements

We thank Yingyu Hu and Rosie Sheward for help with sampling and Yue Liang for help with early analysis. This work was supported by the National Natural Science Foundation of China (32001180 (ZL)), the Natural Sciences and Engineering Research Council of Canada (NSERC) Discovery (ZVF, AJI), Canada Research Chairs (ZVF) program, and the Simons Collaboration on Computational Biogeochemical Modeling of Marine Ecosystems/CBIOMES (grant nos: 549937 (ZVF) and 549935 (AJI)).

Competing interests

None declared.

Author contributions

ZL and ZVF designed research. ZL, YZ and WL performed the experiments, ZL performed the bioinformatics analysis. ZL, AJI and ZVF wrote the paper. All authors contributed to the corrections of the manuscript.

ORCID

Zoe V. Finkel  <https://orcid.org/0000-0003-4212-3917>
 Andrew J. Irwin  <https://orcid.org/0000-0001-7784-2319>
 Wei Li  <https://orcid.org/0000-0002-4127-8311>
 Zhongke Li  <https://orcid.org/0000-0001-8735-2313>
 Yong Zhang  <https://orcid.org/0000-0001-8805-1205>

Data availability

The data that support the findings of this study are available in the [Supporting Information](#) of this article (Figs S1–S19; Tables S1, S2; Datasets S1–S7). The sequencing data of RNA-Seq of this study are available through NCBI SRA (BioProject: PRJNA734969).

References

- Abida H, Dolch LJ, Mei C, Villanova V, Conte M, Block MA, Finazzi G, Bastien O, Tirichine L, Bowler C. 2015. Membrane glycerolipid remodeling triggered by nitrogen and phosphorus starvation in *Phaeodactylum tricornutum*. *Plant Physiology* 167: 118–136.
- Aiken CT, Kaake RM, Wang X, Huang L. 2011. Oxidative stress-mediated regulation of proteasome complexes. *Molecular & Cellular Proteomics* 10: R110.006924.
- Alexander H, Jenkins BD, Ryneerson TA, Dyhrman ST. 2015. Metatranscriptome analyses indicate resource partitioning between diatoms in the field. *Proceedings of the National Academy of Sciences, USA* 112: E2182–E2190.
- Alipanah L, Rohloff J, Winge P, Bones AM, Brembu T. 2015. Whole-cell response to nitrogen deprivation in the diatom *Phaeodactylum tricornutum*. *Journal of Experimental Botany* 66: 6281–6296.
- Allen AE, LaRoche J, Maheswari U, Lommer M, Schauer N, Lopez PJ, Finazzi G, Fernie AR, Bowler C. 2008. Whole-cell response of the pennate diatom *Phaeodactylum tricornutum* to iron starvation. *Proceedings of the National Academy of Sciences, USA* 105: 10438–10443.
- Andrews S. 2010. *FASTQC: a quality control tool for high throughput sequence data*. Cambridge, UK: Babraham Bioinformatics, Babraham Institute.
- Armbrust EV, Berges JA, Bowler C, Green BR, Martinez D, Putnam NH, Zhou S, Allen AE, Apt KE, Bechner M. 2004. The genome of the diatom *Thalassiosira pseudonana*: ecology, evolution, and metabolism. *Science* 306: 79–86.
- Bard JA, Goodall EA, Greene ER, Jonsson E, Dong KC, Martin A. 2018. Structure and function of the 26S proteasome. *Annual Review of Biochemistry* 87: 697–724.
- Becker KW, Harke MJ, Mende DR, Muratore D, Weitz JS, DeLong EF, Dyhrman ST, Van Mooy BA. 2021. Combined pigment and metatranscriptomic analysis reveals highly synchronized diel patterns of phenotypic light response across domains in the open oligotrophic ocean. *The ISME Journal* 15: 520–533.
- Benjamini Y, Hochberg Y. 1995. Controlling the false discovery rate: a practical and powerful approach to multiple testing. *Journal of the Royal Statistical Society: Series B (Methodological)* 57: 289–300.
- Berges JA, Franklin DJ, Harrison PJ. 2001. Evolution of an artificial seawater medium: improvements in enriched seawater, artificial water over the last two decades. *Journal of Phycology* 37: 1138–1145.
- Bolger AM, Lohse M, Usadel B. 2014. TRIMMOMATIC: a flexible trimmer for Illumina sequence data. *Bioinformatics* 30: 2114–2120.
- Borowitzka MA. 2018. The ‘stress’ concept in microalgal biology – homeostasis, acclimation and adaptation. *Journal of Applied Phycology* 30: 2815–2825.
- Boyd PW, Collins S, Dupont S, Fabricius K, Gattuso J-P, Havenhand J, Hutchins DA, McGraw CM, Riebesell U, Vichi M. 2019. *SCOR WG149 handbook to support the SCOR best practice guide for ‘multiple drivers’ marine research*. Hobart, Tas., Australia: University of Tasmania, on behalf of Scientific Committee on Oceanic Research (SCOR).
- Causton HC, Ren B, Koh SS, Harbison CT, Kanin E, Jennings EG, Lee TI, True HL, Lander ES, Young RA. 2001. Remodeling of yeast genome expression in response to environmental changes. *Molecular Biology of the Cell* 12: 323–337.
- Chen D, Toone WM, Mata J, Lyne R, Burns G, Kivinen K, Brazma A, Jones N, Bähler J. 2003. Global transcriptional responses of fission yeast to environmental stress. *Molecular Biology of the Cell* 14: 214–229.
- Crespo JL, Hall MN. 2002. Elucidating TOR signaling and rapamycin action: lessons from *Saccharomyces cerevisiae*. *Microbiology and Molecular Biology Reviews* 66: 579–591.
- Cruz de Carvalho MH, Sun H-X, Bowler C, Chua N-H. 2016. Noncoding and coding transcriptome responses of a marine diatom to phosphate fluctuations. *New Phytologist* 210: 497–510.
- Davies KJ. 2001. Degradation of oxidized proteins by the 20S proteasome. *Biochimie* 83: 301–310.
- De Geyter N, Gholami A, Goormachtig S, Goossens A. 2012. Transcriptional machineries in jasmonate-elicited plant secondary metabolism. *Trends in Plant Science* 17: 349–359.
- De La Rocha CL, Passow U. 2004. Recovery of *Thalassiosira weissflogii* from nitrogen and silicon starvation. *Limnology and Oceanography* 49: 245–255.
- Dobrenel T, Caldana C, Hanson J, Robaglia C, Vincentz M, Veit B, Meyer C. 2016. TOR signaling and nutrient sensing. *Annual Review of Plant Biology* 67: 261–285.
- Dyhrman ST, Jenkins BD, Ryneerson TA, Saito MA, Mercier ML, Alexander H, Whitney LP, Drzewianowski A, Bulygin VV, Bertrand EM. 2012. The transcriptome and proteome of the diatom *Thalassiosira pseudonana* reveal a diverse phosphorus stress response. *PLoS ONE* 7: e33768.
- Ewels P, Magnusson M, Lundin S, Käller M. 2016. MULTIQC: summarize analysis results for multiple tools and samples in a single report. *Bioinformatics* 32: 3047–3048.
- Falkowski PG, Barber RT, Smetacek V. 1998. Biogeochemical controls and feedbacks on ocean primary production. *Science* 281: 200–206.
- Field CB, Behrenfeld MJ, Randerson JT, Falkowski P. 1998. Primary production of the biosphere: integrating terrestrial and oceanic components. *Science* 281: 237–240.
- Gasch AP, Spellman PT, Kao CM, Carmel-Harel O, Eisen MB, Storz G, Botstein D, Brown PO. 2000. Genomic expression programs in the response of yeast cells to environmental changes. *Molecular Biology of the Cell* 11: 4241–4257.
- Gill SS, Tuteja N. 2010. Reactive oxygen species and antioxidant machinery in abiotic stress tolerance in crop plants. *Plant Physiology and Biochemistry* 48: 909–930.
- Gillooly JF, Brown JH, West GB, Savage VM, Charnov EL. 2001. Effects of size and temperature on metabolic rate. *Science* 293: 2248–2251.
- González A, Hall MN. 2017. Nutrient sensing and TOR signaling in yeast and mammals. *EMBO Journal* 36: 397–408.
- Harper JW, Bennett EJ. 2016. Proteome complexity and the forces that drive proteome imbalance. *Nature* 537: 328–338.
- Hennon GM, Ashworth J, Groussman RD, Berthiaume C, Morales RL, Baliga NS, Orellana MV, Armbrust EV. 2015. Diatom acclimation to elevated CO₂ via cAMP signalling and coordinated gene expression. *Nature Climate Change* 5: 761–765.
- Hockin NL, Mock T, Mulholland F, Kopriva S, Malin G. 2012. The response of diatom central carbon metabolism to nitrogen starvation is different from that of green algae and higher plants. *Plant Physiology* 158: 299–312.
- Huner NP, Öquist G, Sarhan F. 1998. Energy balance and acclimation to light and cold. *Trends in Plant Science* 3: 224–230.
- Järvi S, Suorsa M, Aro E-M. 2015. Photosystem II repair in plant chloroplasts—regulation, assisting proteins and shared components with photosystem II biogenesis. *Biochimica et Biophysica Acta (BBA)-Bioenergetics* 1847: 900–909.
- Jones CB, Ott EM, Keener JM, Curtiss M, Sandrin V, Babst M. 2012. Regulation of membrane protein degradation by starvation-response pathways. *Traffic* 13: 468–482.
- Karp PD, Midford PE, Caspi R, Khodursky A. 2021. Pathway size matters: the influence of pathway granularity on over-representation (enrichment analysis) statistics. *BMC Genomics* 22: 1–11.
- Kolde R. 2012. *PHEATMAP: pretty heatmaps*. R package v.1.0.12. [WWW document] URL <https://CRAN.R-project.org/package=pheatmap> [accessed 12 June 2022].
- Kwon YT, Ciechanover A. 2017. The ubiquitin code in the ubiquitin-proteasome system and autophagy. *Trends in Biochemical Sciences* 42: 873–886.
- Lang MJ, Martinez-Marquez JY, Prosser DC, Ganser LR, Buelto D, Wendland B, Duncan MC. 2014. Glucose starvation inhibits autophagy via vacuolar

- hydrolysis and induces plasma membrane internalization by down-regulating recycling. *Journal of Biological Chemistry* 289: 16736–16747.
- Levitán O, Dinamarca J, Zelzion E, Lun DS, Guerra LT, Kim MK, Kim J, Van Mooy BA, Bhattacharya D, Falkowski PG. 2015. Remodeling of intermediate metabolism in the diatom *Phaeodactylum tricornerutum* under nitrogen stress. *Proceedings of the National Academy of Sciences, USA* 112: 412–417.
- Li Y, Zhuang S, Wu Y, Ren H, Cheng F, Lin X, Wang K, Beardall J, Gao K. 2015. Ocean acidification modulates expression of genes and physiological performance of a marine diatom. *Biogeosciences Discussions* 12: 15809–15833.
- Li Z, Li W, Zhang Y, Hu Y, Sheward R, Irwin AJ, Finkel ZV. 2020. Dynamic photophysiological stress response of a model diatom to ten environmental stresses. *Journal of Phycology* 57: 484–495.
- Li Z, Zhang Y, Li W, Irwin AJ, Finkel ZV. 2022. Conservation and architecture of housekeeping genes in the model marine diatom *Thalassiosira pseudonana*. *New Phytologist* 234: 1363–1376.
- Liang Y, Koester JA, Liefer JD, Irwin AJ, Finkel ZV. 2019. Molecular mechanisms of temperature acclimation and adaptation in marine diatoms. *The ISME Journal* 13: 2415–2425.
- Lin S-C, Hardie DG. 2018. AMPK: sensing glucose as well as cellular energy status. *Cell Metabolism* 27: 299–313.
- Lin X, Tirichine L, Bowler C. 2012. Protocol: chromatin immunoprecipitation (ChIP) methodology to investigate histone modifications in two model diatom species. *Plant Methods* 8: 1–9.
- Love MI, Huber W, Anders S. 2014. Moderated estimation of fold change and dispersion for RNA-seq data with DESeq2. *Genome Biology* 15: 550.
- MacGurn JA, Hsu P-C, Smolka MB, Emr SD. 2011. TORC1 regulates endocytosis via Npr1-mediated phosphoinhibition of a ubiquitin ligase adaptor. *Cell* 147: 1104–1117.
- Martin-Jézéquel V, Hildebrand M, Brzezinski MA. 2000. Silicon metabolism in diatoms: implications for growth. *Journal of Phycology* 36: 821–840.
- Mathis AD, Naylor BC, Carson RH, Evans E, Harwell J, Knecht J, Hexem E, Peeler FF, Miller BF, Hamilton KL. 2017. Mechanisms of *in vivo* ribosome maintenance change in response to nutrient signals. *Molecular & Cellular Proteomics* 16: 243–254.
- Maxwell DP, Falk S, Trick CG, Huner NP. 1994. Growth at low temperature mimics high-light acclimation in *Chlorella vulgaris*. *Plant Physiology* 105: 535–543.
- Mock T, Samanta MP, Iverson V, Berthiaume C, Robison M, Holtermann K, Durkin C, BonDurant SS, Richmond K, Rodesch M. 2008. Whole-genome expression profiling of the marine diatom *Thalassiosira pseudonana* identifies genes involved in silicon bioprocesses. *Proceedings of the National Academy of Sciences, USA* 105: 1579–1584.
- Müller M, Schmidt O, Angelova M, Faserl K, Weys S, Kremser L, Pfaffenwimmer T, Dalik T, Kraft C, Trajanoski Z. 2015. The coordinated action of the MVB pathway and autophagy ensures cell survival during starvation. *eLife* 4: e07736.
- Muratore D, Boysen AK, Härke MJ, Becker KW, Casey JR, Coesel SN, Mende DR, Wilson ST, Aylward FO, Eppley JM. 2022. Complex marine microbial communities partition metabolism of scarce resources over the diel cycle. *Nature Ecology & Evolution* 6: 218–229.
- Nisbet RER, Kilian O, McFadden GI. 2004. Diatom genomics: genetic acquisitions and mergers. *Current Biology* 14: R1048–R1050.
- Nymark M, Valle KC, Brembu T, Hancke K, Winge P, Andresen K, Johnsen G, Bones AM. 2009. An integrated analysis of molecular acclimation to high light in the marine diatom *Phaeodactylum tricornerutum*. *PLoS ONE* 4: e7743.
- Oudot-Le Secq M-P, Grimwood J, Shapiro H, Armbrust EV, Bowler C, Green BR. 2007. Chloroplast genomes of the diatoms *Phaeodactylum tricornerutum* and *Thalassiosira pseudonana*: comparison with other plastid genomes of the red lineage. *Molecular Genetics and Genomics* 277: 427–439.
- Park S, Jung G, Hwang Y, Jin E. 2010. Dynamic response of the transcriptome of a psychrophilic diatom, *Chaetoceros neogracile*, to high irradiance. *Planta* 231: 349–360.
- Patro R, Duggal G, Love MI, Irizarry RA, Kingsford C. 2017. Salmon provides fast and bias-aware quantification of transcript expression. *Nature Methods* 14: 417–419.
- Pérez-Pérez ME, Couso I, Crespo JL. 2017. The TOR signaling network in the model unicellular green alga *Chlamydomonas reinhardtii*. *Biomolecules* 7: 54.
- Pfannschmidt T, Nilsson A, Allen JF. 1999. Photosynthetic control of chloroplast gene expression. *Nature* 397: 625–628.
- Pietrocola F, Galluzzi L, Bravo-San Pedro JM, Madeo F, Kroemer G. 2015. Acetyl coenzyme A: a central metabolite and second messenger. *Cell Metabolism* 21: 805–821.
- Pogson BJ, Woo NS, Förster B, Small ID. 2008. Plastid signalling to the nucleus and beyond. *Trends in Plant Science* 13: 602–609.
- Prihoda J, Tanaka A, de Paula WB, Allen JF, Tirichine L, Bowler C. 2012. Chloroplast-mitochondria cross-talk in diatoms. *Journal of Experimental Botany* 63: 1543–1557.
- Puchalska P, Crawford PA. 2017. Multi-dimensional roles of ketone bodies in fuel metabolism, signaling, and therapeutics. *Cell Metabolism* 25: 262–284.
- Pulk A, Liiv A, Peil L, Maiväli Ü, Nierhaus K, Remme J. 2010. Ribosome reactivation by replacement of damaged proteins. *Molecular Microbiology* 75: 801–814.
- R Development Core Team. 2013. R: A language and environment for statistical computing, v.4.2.0. [WWW document] URL www.r-project.org [accessed 22 April 2022].
- Raven JA, Geider RJ. 1988. Temperature and algal growth. *New Phytologist* 110: 441–461.
- Remmers IM, D'Adamo S, Martens DE, de Vos RC, Mumm R, America AH, Cordewener JH, Bakker LV, Peters SA, Wijffels RH. 2018. Orchestration of transcriptome, proteome and metabolome in the diatom *Phaeodactylum tricornerutum* during nitrogen limitation. *Algal Research* 35: 33–49.
- Rexin D, Meyer C, Robaglia C, Veit B. 2015. TOR signalling in plants. *Biochemical Journal* 470: 1–14.
- Sapriel G, Quinet M, Heijde M, Jourden L, Tanty V, Luo G, Le Crom S, Lopez PJ. 2009. Genome-wide transcriptome analyses of silicon metabolism in *Phaeodactylum tricornerutum* reveal the multilevel regulation of silicic acid transporters. *PLoS ONE* 4: e7458.
- Schleif R. 1967. Control of production of ribosomal protein. *Journal of Molecular Biology* 27: 41–55.
- Shang F, Taylor A. 2011. Ubiquitin–proteasome pathway and cellular responses to oxidative stress. *Free Radical Biology and Medicine* 51: 5–16.
- Sharma P, Jha AB, Dubey RS, Pessarakli M. 2012. Reactive oxygen species, oxidative damage, and antioxidative defense mechanism in plants under stressful conditions. *Journal of Botany* 2012: 1–26.
- Shi L, Tu BP. 2015. Acetyl-CoA and the regulation of metabolism: mechanisms and consequences. *Current Opinion in Cell Biology* 33: 125–131.
- Shrestha RP, Tesson B, Norden-Krichmar T, Federowicz S, Hildebrand M, Allen AE. 2012. Whole transcriptome analysis of the silicon response of the diatom *Thalassiosira pseudonana*. *BMC Genomics* 13: 499.
- Smith SR, Glé C, Abbriano RM, Traller JC, Davis A, Trentacoste E, Vernet M, Allen AE, Hildebrand M. 2016. Transcript level coordination of carbon pathways during silicon starvation-induced lipid accumulation in the diatom *Thalassiosira pseudonana*. *New Phytologist* 210: 890–904.
- Takahashi S, Murata N. 2008. How do environmental stresses accelerate photoinhibition? *Trends in Plant Science* 13: 178–182.
- Timmis JN, Ayliffe MA, Huang CY, Martin W. 2004. Endosymbiotic gene transfer: organelle genomes forge eukaryotic chromosomes. *Nature Reviews Genetics* 5: 123–135.
- Tréguer P, Bowler C, Moriceau B, Dutkiewicz S, Gehlen M, Aumont O, Bittner L, Dugdale R, Finkel Z, Iudicone D. 2018. Influence of diatom diversity on the ocean biological carbon pump. *Nature Geoscience* 11: 27–37.
- Warner JR. 1999. The economics of ribosome biosynthesis in yeast. *Trends in Biochemical Sciences* 24: 437–440.
- Wickham H. 2016. ggplot2: elegant graphics for data analysis. R package v.3.3.6. [WWW document] URL <https://cran.r-project.org/web/packages/ggplot2/index.html> [accessed 12 June 2022].
- Wingett SW, Andrews S. 2018. FASTQ SCREEN: a tool for multi-genome mapping and quality control. *F1000Research* 7: 1338.
- Xiong Y, Sheen J. 2015. Novel links in the plant TOR kinase signaling network. *Current Opinion in Plant Biology* 28: 83–91.
- Zhang S-F, Yuan C-J, Chen Y, Chen X-H, Li D-X, Liu J-L, Lin L, Wang D-Z. 2016. Comparative transcriptomic analysis reveals novel insights into the adaptive response of *Skeletonema costatum* to changing ambient phosphorus. *Frontiers in Microbiology* 7: 1476.

Supporting Information

Additional Supporting Information may be found online in the Supporting Information section at the end of the article.

Dataset S1 Description of raw read files.

Dataset S2 Annotations and the differential expression (\log_2FC) of the differentially expressed genes (including diatom environmental stress response genes, genes linked to reactive oxygen stress, and weighted gene correlation network analysis module genes).

Dataset S3 Differential expression (\log_2FC) of the differentially expressed Kyoto Encyclopedia of Genes and Genomes Orthologs.

Dataset S4 Kyoto Encyclopedia of Genes and Genomes enrichment under different stressors.

Dataset S5 Transcripts per million values of genes in all sequenced samples gene annotation.

Dataset S6 Enrichment analysis of diatom environmental stress response genes listing the significantly (P -valueAdj and P -value < 0.01) enriched pathways or terms, their pathway, and descriptions.

Dataset S7 Count of diatom environmental stress response genes in Kyoto Encyclopedia of Genes and Genomes pathways.

Fig. S1 Mapping rate of RNA-Seq samples.

Fig. S2 Counts of the differentially expressed genes across selected environmental stressors and time treatments.

Fig. S3 Analysis of the diatom environmental stress response genes with unknown function.

Fig. S4 Kyoto Encyclopedia of Genes and Genomes pathways in the diatom environmental stress response.

Fig. S5 Comparison of the common set of genes induced by both Si starvation and Fe starvation in Mock *et al.* (2008) and this study.

Fig. S6 Pairwise Spearman correlations across 40 treatments and sampling times of the median differential expression of Kyoto Encyclopedia of Genes and Genomes Orthologs between 84 enriched pathways.

Fig. S7 Differential expression of genes in pathways of DNA replication and nucleic acid metabolism under 10 environmental stressors.

Fig. S8 Differential expression of genes in central carbon metabolic pathways under 10 environmental stressors.

Fig. S9 Differential expression of genes in lipid-related pathways under 10 environmental stressors.

Fig. S10 Differential expression of genes in 12 proteome-balance-related pathways.

Fig. S11 Differential expression of genes related to photosynthesis under 10 environmental stressors in nine functional categories.

Fig. S12 Differential expression of genes in global regulatory pathways under 10 environmental stressors.

Fig. S13 Linear correlation between median differential expression of genes in the valine, leucine, and isoleucine degradation pathway and other pathways across 40 observations.

Fig. S14 Differential expression of transcription factors that are identified as diatom environmental stress response genes in this study.

Fig. S15 Weighted gene correlation network analysis showing co-expression patterns and possible regulatory mechanisms.

Fig. S16 Overrepresented motifs detected using promoters of genes in each module as a training set.

Fig. S17 Comparison of the differential expression of common environmental stress response genes in *Saccharomyces cerevisiae* and their orthologs in *Thalassiosira pseudonana*.

Fig. S18 Re-clustering of microarray differential expression data of *Saccharomyces cerevisiae* under different stressors.

Fig. S19 Differential expression of genes in glutathione metabolism pathway (ko00480) under 10 environmental stressors.

Table S1 Experimental set-up for each treatment.

Table S2 Numbers of genes and pathways in the diatom environmental stress response for all genes and pathways, for genes linked to protein homeostasis, and for genes linked to oxidative stress by the reactive oxygen stress treatment.

Please note: Wiley is not responsible for the content or functionality of any Supporting Information supplied by the authors. Any queries (other than missing material) should be directed to the *New Phytologist* Central Office.